acta physica slovaca vol. 54 No. 4, 375 – 384 **August 2004**

CHARGED HADRONS AND LEPTONS IDENTIFICATION AT HADES

A. Kugler*[,1], H. Agakishiev[2], C. Agodi[3], H. Alvarez-Pol[4], A. Balanda[5], G. Bellia[3,6], J. Bielčik[2], M. Böhmer[7], J. Boyard[8], P. Braun-Munzinger[2], S. Chernenko[9], T. Christ[7], R. Coniglione[3], R. Djeridi[10], F. Dohrmann[11], I. Duran[4], Th. Eberl[7], L. Fabbietti[7], O. Fateev[9], P. Finocchiaro[3], J. Friese[7], I. Fröhlich[10], J. Garzon[4], R. Gernhäuser[7], M. Golubeva[12], D. Gonzales-Dias[4], E. Grosse[11], F. Guber[12], T. Hennino[8], S. Hlaváč[13], R. Holzmann[2], A. Ierusalimov[9], I. Iori[14,15], M. Jaskula[5], M.Jurkovi[7], B. Kämpfer[11], K. Kanaki[11], T. Karavicheva[12] , I. Koenig[2], W. Koenig[2], B. Kolb[2], R. Kotte[11], J. Kotulič-Bunta[13], R. Krücken[7], W. Kühn[10], R. Kulessa[5], A. Kurepin[12], S. Lang[2], J. Lehnert[10], C. Maiolino[3], J. Markert[16], V. Metag[10], J. Mousa[17], M. Münch[7], C. Müntz[16], L. Naumann[11], R. Novotny[10], J. Novotný[1], J. Otwinowski[5], Y. Pachmayer[16], V. Pechenov[9], T. Perez[10], J. Pietraszko[5], R. Pleskač[1], V. Pospíšil[1], W. Przygoda[5], N. Rabin[18], B. Ramstein[8], A. Reshetin[12], J. Ritman[10], M. Roy-Stephan[8], A. Rustamov[2], A. Sadovski[11], B. Sailer[7], P. Salabura[5], M. Sanchez[4], P. Sapienza[3], A. Schmah[2], R. Simon[2], V. Smoliankin[18], L. Smykov[9] , S. Spataro[3], B. Spruck[10], H. Ströbele[16], J. Stroth[2,16], C. Sturm[2], M. Sudol[2], P. Tlustý[1], A. Toia[10], M. Traxler[10], H. Tsertos[17], V. Wagner[1], M. Wiśniowski[5], T. Wojcik[5], J. Wüstenfeld[16], Yu. Zanevsky[9], D. Žovinec[13], P. Zumbruch[2]

[1] *Nuclear Physics Institute, Czech Academy of Sciences, 25068 Řež, Czech Republic*
[2] *Gesellschaft fur Schwerionenforschung , 64220 Darmstadt, Germany*
[3] *Istituto Nazionale di Fisica Nucleare - Laboratori Nazionali del Sud, 95125 Catania, Italy*
[4] *Departamento de Fisica de Particulas, University of Santiago de Compostela, 15706 Santiago de Compostela, Spain*
[5] *Smoluchowski Institute of Physics, Jagiellonian University of Cracow, 30059 Cracow, Poland*
[6] *Dipartimento di Fisica, Università di Catania, 95125, Catania, Italy*
[7] *Physik Department E12, Technische Universität München, 85748 Garching, Germany*
[8] *Institut de Physique Nucléaire d'Orsay, CNRS/IN2P3, 91406 Orsay Cedex, France*
[9] *Joint Institute of Nuclear Research, 141980 Dubna, Russia*
[10] *II.Physikalisches Institut, Justus Liebig Universität Giessen, 35392 Giessen, Germany*
[11] *Institut für Kern- und Hadronenphysik, Forschungszentrum Rossendorf, PF 510119, 01314 Dresden, Germany*
[12] *Institute for Nuclear Research, Russian Academy of Science, Moscow, 117259 Moscow, Russia*
[13] *Institute of Physics, Slovak Academy of Sciences, 84511 Bratislava, Slovakia*
[14] *Istituto Nazionale di Fisica Nucleare, Sezione di Milano, 20133 Milano, Italy*
[15] *Dipartimento di Fisica, Università di Milano, 20133 Milano, Italy*

*E-mail address: kugler@ujf.cas.cz

0323-0465/04

[16] Institut für Kernphysik, Johann Wolfgang Goethe-Universität, 60486 Frankfurt, Germany
[17] Department of Physics, University of Cyprus, 1678 Nicosia, Cyprus
[18] Institute of Theoretical and Experimental Physics, 117259 Moscow, Russia

Received 6 April 2004, accepted 28 June 2004

The HADES spectrometer installed at GSI Darmstadt is devoted to the study of the production of di-lepton pairs from vector meson decays in relativistic nucleus-nucleus collisions, as well as proton- and pion-induced reactions. Extraction of rare lepton pairs in high hadron multiplicity events requires an efficient particle identification (PID). In HADES charged particles momentum is measured by a tracking system surrounding the toroidal super conducting magnet, and velocity and energy loss is provided by a TOF detector. Leptons are identified by a Rich as well as a Shower detector. The particle identification method is using full experimental information from all subdetectors. To demonstrate the method performance, single particle spectra of charged hadrons and leptons from C+C at $2A$ GeV will be presented and compared with results of corresponding simulations. The proton and pion yields an m_{T} and rapidity distributions will be compared with existing data. Very preliminary results of lepton analysis will be shown as well.

PACS: 25.75.-q, 25.75DW, 29.30Aj

1 Introduction

During last decade significant enhancements of di-lepton yields in invariant mass spectra, as compared to an appropriate superposition of di-lepton contributions from freely decaying hadrons, were found both at relativistic (1-2A GeV) [1] and ultra-relativistic (160-200A GeV) heavy ion collisions [2]. In the intermediate mass range (200 MeV/c^2 $< M_{\mathrm{inv}} <$ 500 MeV/c^2) below the pole mass of the short lived ρ-meson, the yield exceeds standard theoretical predictions up to a factor 5-7. Presently most of the theoretical studies interpret these findings as a possible manifestation of the change of the vector mesons properties inside the nuclear medium. However, the underlying phenomenon could not be identified unambiguously and various interpretations have been proposed [3]. A new round of experiments aiming at better mass resolution and statistics is now under way to provide more precise data [4]. The High Acceptance Di-Electron Spectrometer (HADES) is a new second-generation di-electron spectrometer designed to operate with proton, pion and heavy ion beams provided by the GSI accelerator facility in Darmstadt [5]. The spectrometer was built during 1997-2003 and is presently becoming operational. In this paper we present first results concerning the particle identification capabilities of the spectrometer, for further details see [6].

2 The Spectrometer

The HADES spectrometer is schematically depicted in Fig. 1. A fast hadron-blind Ring Imaging Cherenkov (RICH) counter with gas radiator and solid CsI photocathode, placed around a segmented target, is used for electron identification [7]. Four Multi-wire Drift Chambers (MDC1-MDC4) together with a superconducting magnet, form the magnetic spectrometer for momentum

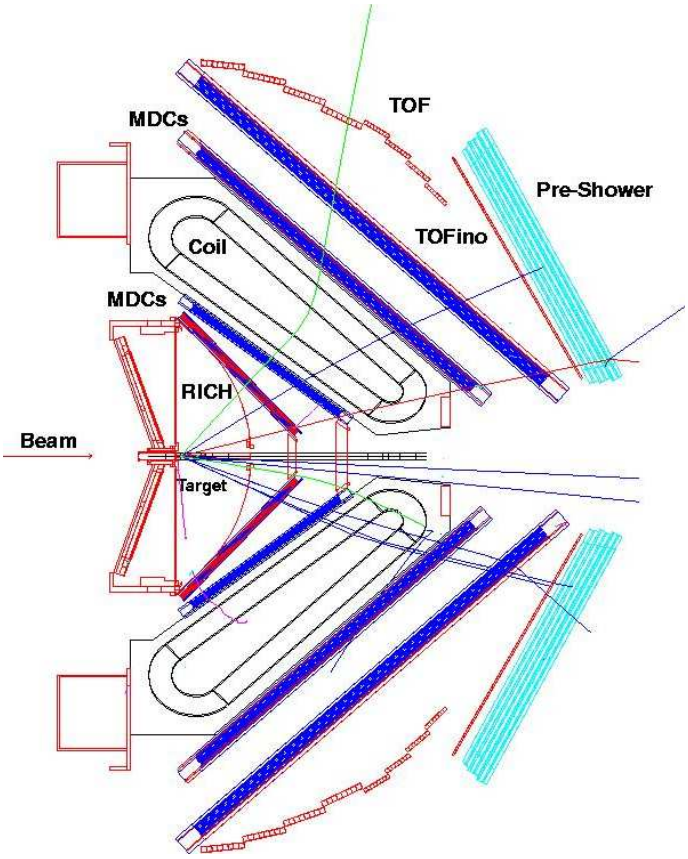

Fig. 1. Schematic cross section of the HADES spectrometer.

measurement with an expected invariant mass resolution of 1-2% in the ρ/ω region [8]. A set of electromagnetic Pre-Shower detectors, together with a TOFINO ($18^\circ < \theta < 45^\circ$ and a Time-Of-Flight (TOF, $45^\circ < \theta < 85^\circ$) scintillator walls, constitute the Multiplicity and Electron Trigger Array (META) [9]. Each of above mentioned sub-detectors consists of six segments surrounding the target. A fast data acquisitions system is used as well as a two-level trigger scheme [10]: (a) LVL1 – fast determination of the charged particle multiplicity ($M_{\rm ch}$) in the META, in order to select central collisions and thus provide a first level trigger; (b) LVL2 – real time selection of electron pairs within a selectable invariant mass window, by correlating the impact position of each fast particle detected in the META with the center of a corresponding ring detected in the RICH. In this report we present results from a commissioning run in November 2001, where the HADES detector was operated using only the following sub-systems: the RICH, the two inner MDC planes and the outer META. One of the studied reactions was C+C at $2A$ GeV. The intensity of the beam was $I_{\rm beam} = 10^6$ particles/s and a 5% interaction length target was used. We collected 8x10^7LVL1 triggered events with $M_{\rm ch} > 3$. The MDC track

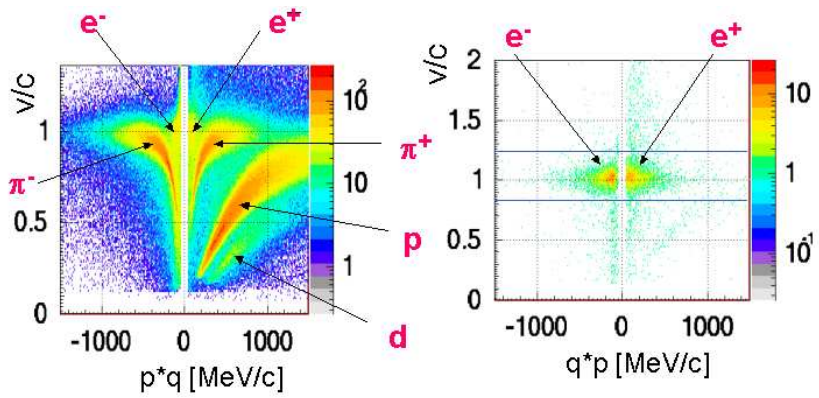

Fig. 2. Left: velocity versus sign(charge)*momentum correlation for all reconstructed tracks from C+C at 2A GeV collisions. Pion and proton branches are clearly resolved. Right: same as on the left but with additional condition on electron identification. Intensity scale is logarithmic.

segments were correlated with corresponding hits in the META after the magnetic field, in order to determine the momentum of particles. Simulation events were generated by a UrQMD code, while the propagation of particles and the detector response was simulated using a Geant 3 based package including the full HADES geometry. After digitization of the simulated information the resulting simulation data were analyzed in the same way as the experimental data.

3 Charged hadrons

Hadron identification is performed mainly on the basis of the measured momentum, velocity and energy loss in the TOF detector. The principle of the hadron identification is illustrated in Fig 2. Particles with different mass fill different regions in the velocity vs. momentum distribution. The pronounced maxima correspond to positive/negative pions and protons. One can also appreciate the effect of the superior time resolution of the TOF detector ($\sigma_{\rm tof} \approx 150$ ps) which allows clear separation of charged pions from protons well above 1000 MeV/c transverse momenta. However, at small polar angles ($18^\circ < \theta < 45^\circ$) where a set of electromagnetic Pre-Shower detectors, together with a TOFINO is used, much worse time resolution of the TOFINO ($\sigma_{\rm tofino} \approx 450$ ps) limits efficient separation of charged pions from protons to momenta below 1000 MeV/c.

A particle identification method has been adopted, which allows efficient identification of particles, using full experimental information from all subdetectors [11]. The basis of the method is a test of the hypothesis, that the reconstructed track with a given momentum can be identified as certain particle specie (e.g. as proton, π meson, electron etc.). Several measured variables from various subdetectors are associated to each identified track. The method incorporates full experimental information in terms of a probability calculations. The probability distribution of each variable for each possible particle type (probability density function) has to be known and parametrized. For the resulting PID probability calculation the Bayesian approach is imple-

mented taking into account the prior abundance of individual particle types, as well as the known detector response. The performance of the method – in terms of efficiency and purity – is then evaluated in detailed simulations.

The first step in the PID method is the calculation of the probability density function (p.d.f.) for each particle type. In case of the "BetaVsMom" method the p.d.f. is the probability distribution of velocity. For each type of particles it has been determined as a function of momentum and emission angle. It has been achieved by dividing the two dimensional velocity versus momentum distributions (see Fig. 2) into bins in momentum of suitable size and projecting them onto the velocity axis for each polar angle. The velocity distributions obtained have been fitted by Gaussian curves and by 2^{nd} order polynomial functions for signal and background coming from incorrectly reconstructed tracks (treated as a separate particle type), respectively. For the "ElossVsMom" method, projections onto the "energy loss" axis have been produced in the same way as in the method described above. The energy loss distributions can be fitted by a Landau function.

In the second step the probabilities from individual algorithms are merged. For each particle type, the products of probabilities from all algorithms are calculated and then the Bayes formula is applied to take into account the relative abundances of the particles. Let $\vec{x}$ be a set of k independent HADES observation, p a track momentum and h is a particle hypothesis. If the probability density function in each hypothesis is known, then the likelihood to observe the value $\vec{x} = x_1, x_2, ..., x_k$ of the discriminating variables for the particle hypothesis h is

$$L\left(\vec{x}|h\right) = \prod_k f_k(x_k|p,h), \tag{1}$$

where $f_k(x_k|p,h)$ is the probability that a track with measurement x_k is a particle of species $h = e^+$, e^-, π^+, π^-, K, p, d. In order to calculate the probability $P\left(h|\vec{x}\right)$ that a given track corresponds to the particle type h, the Bayes theorem is used

$$P\left(h|\vec{x}\right) = \frac{L\left(\vec{x}|h\right) \times P\left(h\right)}{\sum\limits_{h=e,K,p,\pi,d} L\left(\vec{x}|h\right) \times P\left(h\right)}, \tag{2}$$

where $P(h)$ is the production probability for particle h a given momentum p and polar angle (relative abundance). The sum of $P\left(h|\vec{x}\right)$ over all particle types h is normalized to 1.

The identification probability P_t^i is defined as

$$P_t^i = \frac{N_t^i}{\sum\limits_j N_t^j}, \tag{3}$$

where i is the identified particle type and t is the true particle type and N_t^i is the number of particles of true type t identified as type i. The true type probability can be written as

$$Q_t^i = \frac{N_t^i}{\sum\limits_s N_s^i}, \tag{4}$$

and the efficiency $\varepsilon_t = P_t^t$ is the probability that a particle with the true type t is identified as the type t. The purity $P^t = Q_t^t$ is the probability that a particle that is identified as the type t is truly

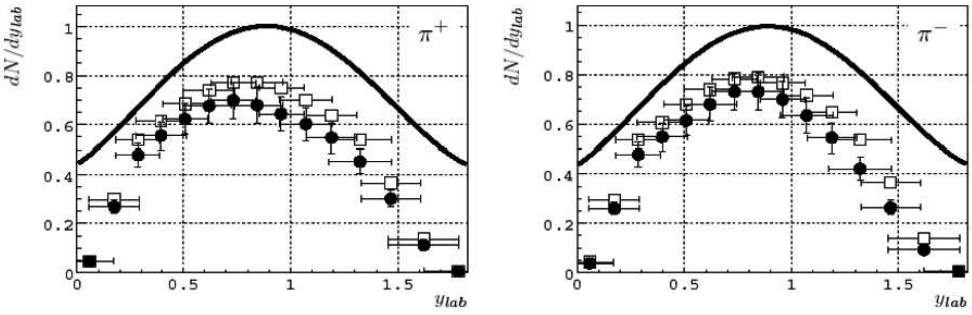

Fig. 3. Rapidity distribution of π mesons. Black circles – experimental data, white squares – simulated data, black line – extrapolation of simulated data to 4π.

of the type t. For instance, P_p^p is the probability that a real proton is identified by the HADES detectors as a proton, and Q_p^p is the probability that a particle that was identified as a proton is truly a proton. The efficiency and the purity are studied with MC simulation data.

The proton, deuteron and pion yields per reaction were extracted from the data using the above described method. The purity of π dentification is 0.7 – 0.9 up to momentum of 1 GeV/c, above this momentum it drops for π^+ because of bad proton – pion separation due to limited time-of-flight resolution of the TOFINO detector. From this reason we limit our analysis on pions to the momentum region below 1000 MeV/c. The efficiency of π dentification is close to 1 in this momentum region. The yields were then corrected on the geometrical acceptance and efficiency of detectors and tracking method. The average correction factor was ~ 0.7. The particle yields per reaction are shown in Tab. 1.

Tab. 1. Yields of particles (per reaction) produced in C + C at $2A$ GeV.

	Within the HADES acceptance	Extrapolated to 4π
π^{r}	0.78	1.27
π^{t}	0.79	1.27
p	3.18	
d	0.31	

While the statistical errors are negligible, the systematical error is estimated as 10%. The main sources of these errors come from inaccuracies of the acceptance correction and the extrapolation of yield to 4π. Averaged number of participants A_{part} in the events selected by the 1^{st} level trigger was estimated using the UrQMD simulations as 8.6. Preliminary pion yield per participant extrapolated to 4π is $N_\pi/A_{\mathrm{part}} = 0.148 \pm 0.015$, where N_π/A_{part} is the averaged yield for positive and negative pions.

The obtained value N_π/A_{part} is in a good agreement with the previous result for the same system and energy measured by the TAPS detector for neutral pions as 0.138 ± 0.014 [12].

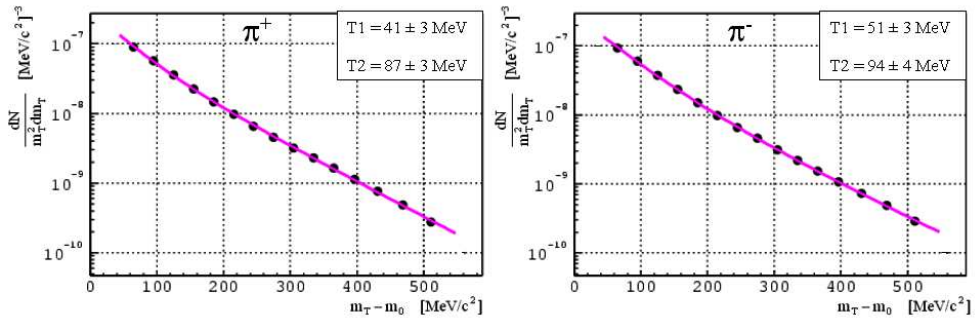

Fig. 4. Transverse mass distribution of π mesons measured at mid-rapidity.

The rapidity and transverse momentum distributions can be used to examine whether the motion of the nucleons is entirely thermal. It will also provide information whether the emitting source is spherical symmetric or elongated and if there is a transverse and longitudinal expansion. Figure 3 shows the rapidity distribution of identified π^+ and π^- for ^{12}C+^{12}C at $2A$ GeV. The distributions exhibit a gaussian-like shape. The centroids and widths of the rapidity distributions from the simulations are in good agreement with the experimental data. The latter can be reproduced assuming a longitudinally expanding thermal source.

In relativistic heavy-ion collisions at 1 – $2A$ GeV the nuclei can be compressed up to about three times the normal nuclear matter density ρ_0 [13]. The hot and dense reaction zone consists of incident nucleons and produced particles. In the thermal model one assumes that the hadronic matter created in nuclear collisions forms an ideal gas. At high internal pressure, the gas expands like a fireball till freeze-out of the hadrons. The measured spectra should exhibit a shape that is expected from a thermal source distribution if the freeze-out process is fast. Information about the degree of equilibration can be obtained from m_{T} spectra measured at mid-rapidity, where $m_{\mathrm{T}} = \sqrt{(p_{\mathrm{T}}^2 + m^2)}$ and p_{T} is the transverse momentum of a particle with mass m. In this case, the particle spectra can be roughly described by a Maxwell-Boltzmann distribution

$$\frac{1}{m_{\mathrm{T}}^2}\frac{\mathrm{d}N}{\mathrm{d}m_{\mathrm{T}}} \propto e^{(-m_{\mathrm{T}}/T)}, \tag{5}$$

where the inverse slope parameter T corresponds to a freeze-out temperature of the particle emitting source.

Figure 4 shows the transverse mass distributions as a function of $(m_{\mathrm{T}} - m_0)$ for π^+ and π^- at midrapidity ($0.8 < y < 1.0$). The solid lines show the results of a thermal fit with two different slopes T_1 and T_2 (see Eq. (6)) that describes the data significantly better as compared to a fit with one slope only.

$$\frac{1}{m_{\mathrm{T}}^2}\frac{\mathrm{d}N}{\mathrm{d}m_{\mathrm{T}}} = C_1 e^{-m_{\mathrm{T}}/T_1} + C_2 e^{-m_{\mathrm{T}}/T_2}. \tag{6}$$

This observation is in agreement with previous results obtained for the same system by the KAOS collaboration. The smaller slope component was interpreted as an indication of a dominant

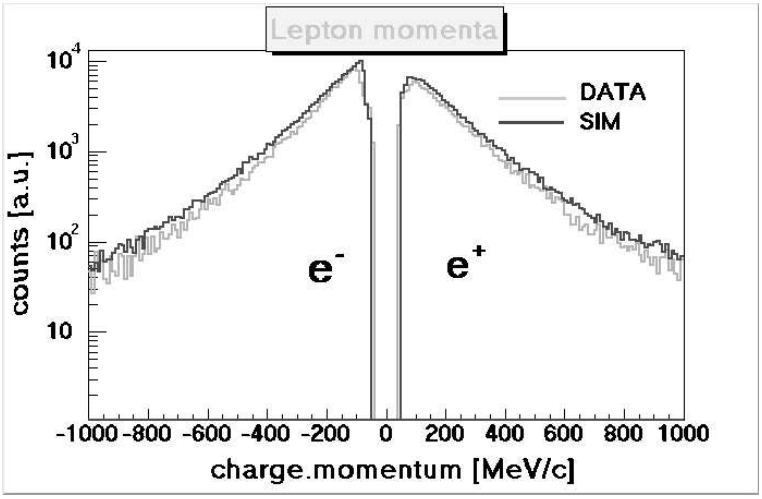

Fig. 5. Momentum spectra electrons detected in C+C at $2A$ GeV compared with results of simulation.

role of Δ resonance in the pion production [14]. The T_1 and T_2 values given in Fig. 4 for π^+ are in good agreement with the results [14], which report $T_1 = 40 \pm 3$ MeV and $T_2 = 86 \pm 3$ MeV. In case of π^- we obtain slightly different values, which may be explained by an imperfect acceptance correction in the mid-rapidity region for low momentum π^- on the border between the TOF and TOFINO detectors ($\theta \approx 45^\circ$).

4 Electrons

For the analysis of electrons the key detector is the RICH. From all the minimum bias reconstructed rings we have chosen suitable quality criteria, in order to suppress fake rings produced for example by electronic noise or charged hadrons traversing the photon detector. The charged particle track segments in the inner MDC were matched with ring centres. The matching condition was $|\Delta\theta| < 1.7^\circ$ and $|\Delta\phi|\sin(\theta) < 1.8^\circ$ for the polar and the azimuthal angles, respectively. Introduction of this matching requirement leads to a drastic reduction of hadronic events, see Fig. 2. For additional electron identification, the following condition on the velocity of particles was applied: $0.8 < \beta < 1.2$ as determined by the TOF and $0.8 < \beta$ by the TOFINO. The β cut in TOFINO has been done only from one side because in case of more than 1 electron hit in a TOFINO paddle, the determination of time is not correct and leads to $\beta > 1.0$ for these cases.

The multiplicity of the identified electrons per event in measured and simulated events differs by less than 30%. The shapes of momentum spectra for electrons and positrons are in both cases very similar (Fig. 5).

From identified unlike sign electrons we have constructed e^+e^- pairs. For further analysis we have used only pairs that contain electron candidates producing different hits in all detectors. Most of them are due to combinatorial background arising from photon conversion and Dalitz decay of π^0 mesons. In order to evaluate the combinatorial background we have used the like-

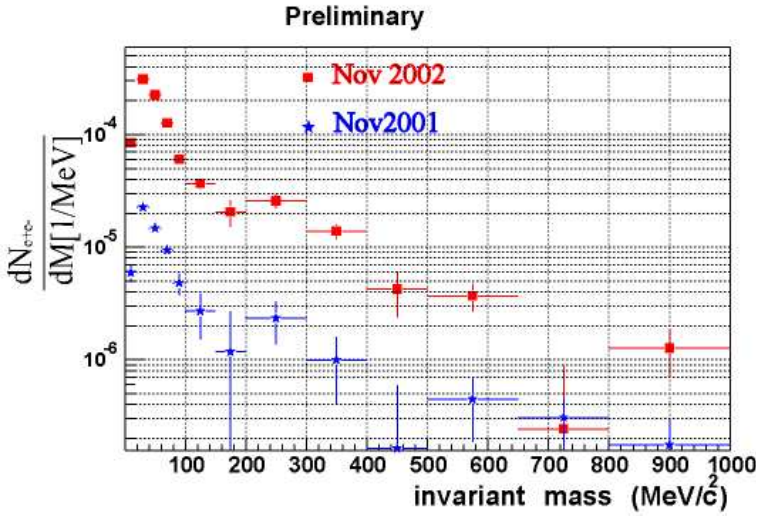

Fig. 6. Comparison of dielectron invariant mass distributions (combinatorial background subtracted) normalized to the number of the LVL1 (stars) and LVL2 (squares) as measured in 2001 and 2002, respectively. Both distributions are preliminary and are not corrected for the detector acceptance and trancking efficiences. Reaction studied was C+C at $2A$ GeV.

sign pairs method [2]. By subtracting from the e+e- spectrum we can get a signal related to di-electron decays. The most dominant sources of e+e- pairs with opening angle larger than 4° are π^0 and, to smaller extent, η Dalitz decays. After subtracting the combinatorial background, we observe indeed that the dominant signal is in the invariant mass region up to 150 MeV/c^2, as expected for π^0 Dalitz decay.

Figure 6 shows a comparison of the signal resulting after the combinatorial background subtraction plotted together for data obtained with LVL1 (stars) and LVL2 (squares) trigger, respectively. The second data set was obtained in the first physics run carried out in November 2002. During this run second level trigger (LVL2) was put into operation for the first time. We studied the C+C reaction at $2A$ GeV beam energy, storing about 213 million events consisting of 56% LVL1 and 44% LVL2 triggers.

Both dilectron distributions were obtained with the same analysis and are for pair opening angle $\theta_{e^+e^-} > 4^\circ$. The spectra have been normalized with the number of collected LVL1 and LVL2 events, respectively, and are not yet corrected for spectrometer acceptance and tracking efficiencies. The impact of the LVL2 clearly results in a strong dielectron statistics enhancement (factor of 10 over run with LVL1 trigger) and allows for investigations of dielectron production over a wider invariant mass range. The analysis is in progress and final results are expected soon.

The data analysis of the Nov2001 run clearly demonstrated the capability of the HADES to identify proton, pions and electron pair signals in a huge hadronic background produced in heavy-ion collisions.

Observed distributions and multiplicities of charged pions confirm previous results obtained

by the TAPS and KAOS collaboration. First dielectron invariant mass distributions were measured in C+C collisions at 2 AGeV in two independent experimental runs. In the second run on-line electron identification (second level trigger) was used for a first time which allowed for a ten-fold increase of dielectron statistics. This data is currently being analyzed and with the results we expect to shed more light on the question of a possible di-electron pair yield excess in the invariant mass region below the ρ/ω vector mesons.

Acknowledgement: This work has been supported by GA CR 202/00/1668 and GA AS CR IAA1048304 and ASCR K1048102 (Czech Republic), KBN 5P03B 140 20 (Poland), BMBF (Germany), INFN (Italy), CNRS/IN2P3 (France), MCYT FPA2000-2041-C02-02 and XUGA PGIDT02PXIC20605PN (Spain), INTAS.

References

[1] R.J. Porter et al.: *Phys. Rev. Lett.* **79** (1997) 1229

[2] Th. Ullrich et al.: *Nucl. Phys. A* **610** (1996) 317c ; A. Drees: *Nucl. Phys. A* **610** (1996) 536c

[3] E.L. Bratkovskaya et al.: *Nucl.Phys. A* **634** (1998) 168 and the references cited therein

[4] H. Appelhauser et al.: *Nucl.Phys. A* **698** (2002) 253c and the references cited therein

[5] A. Kugler: *Czech. J. Phys.* **50/S2** (2000) 72 ; A. Kugler et al.: *Nucl. Phys. A* **734** (2004) 78c

[6] P.Tlusty for the HADES collaboration, *Proceedings of the XLII International Winter Meeting on Nuclear Physics.* Bormio, Ricerca Scientifica ed educazione permanente Vol. S120, (Ed. I. Iori). University of Milano, pp. 171–179; J. Otwinovski et al., in the same volume, pp.180–189

[7] M. Böhmer et al.: *Nucl. Instr. Meth. A* **471** (2001) 25

[8] H. Bokemeyer et al.: *Nucl. Instr. Meth. A* **477** (2002) 397

[9] C. Agodi et al.: *Nucl. Instr. Meth. A* **492** (2002) 14

[10] J. Lehnert at al.: *Nucl. Inst. and Meth. A* **502** (2003) 261 ; A. Toia et al.: *Nucl. Inst. and Meth. A* **502** (2003) 270

[11] R. Barlow et al., *www.slac.stanford.edu/BFROOT/www/Statistics/Report/report.pdf*

[12] R. Averbeck et al.: *Phys. Rev. C* **68** (024903) 2003

[13] W. Busza, A.S. Goldhaber: *Phys. Lett. B* **139** (1984) 235

[14] F. Laue et al.: *Eur. Phys. J. A* **9** (2000) 397